An episodic ataxia type-1 mutation in the S1 segment sensitises the hKv1.1 potassium channel to extracellular Zn^{2+}

Antonella Cusimano[a,1], Maria Cristina D'Adamo[b], Mauro Pessia[b,*]

[a]*Istituto di Ricerche Farmacologiche 'Mario Negri', CMNS, Santa Maria Imbaro (Chieti), Italy*
[b]*Section of Human Physiology, Department of Internal Medicine, University of Perugia School of Medicine, Via del Giochetto, I-06126 Perugia, Italy*

Abstract **Episodic ataxia type-1 (EA1) is a human neurological syndrome characterized by attacks of generalized ataxia and by continuous myokymia that has been associated with point mutations in the voltage-gated potassium channel gene *KCNA1*. Although important advancement has been made in understanding the molecular pathophysiology of EA1, several disease-causing mechanisms remain poorly understood. F184C is an EA1 mutation that is located within the S1 segment of the human Kv1.1 subunit. Here, we show that the F184C mutation increases ~4.5-fold the sensitivity of the channel to extracellular Zn^{2+}. Both Zn^{2+} and Cd^{2+} markedly alter the activation kinetics of F184C channel. In addition, the mutated channel reacts with several methane thiosulfonate reagents which specifically affected channel function. The results provide structural implications and indicate that sensitisation of hKv1.1 to Zn^{2+} is likely to contribute to the EA1 symptoms in patients harboring the F184C mutation.**
© 2004 Federation of European Biochemical Societies. Published by Elsevier B.V. All rights reserved.

Keywords: Voltage-gated potassium channel; Episodic ataxia type-1; *KCNA1*; Zinc; Cadmium

1. Introduction

Episodic ataxia type-1 (EA1) is a rare, autosomal dominant neurological disorder clearly described in 1975 by Van Dyke and co-workers. Affected patients present constant muscle rippling movements (myokymia) and episodic attacks of ataxia. Attacks are characterized by imbalance with jerking movements of the head, arms, legs and can be triggered by emotional stress, fatigue, sudden movements, loud noises, etc. [1–4]. The first symptoms manifest during childhood, persist through the whole life and can vary from severe to no detectable neurological abnormalities. Linkage studies from several EA1 families led to the discovery of a number of point mutations in the voltage-dependent potassium channel gene *KCNA1* (Kv1.1), on chromosome 12p13 [5–8]. The amino acid residues that are mutated in EA1 patients reside at positions highly conserved amongst the delayed-rectifier potassium channel genes [5]. The functional characterization of the mutated channels in *Xenopus* oocytes or mammalian cell lines has demonstrated that EA1 mutations markedly alter the biochemical and biophysical properties of hKv1.1, which result in channels with impaired delayed rectifier function [for reviews see: 9–11].

In their original report, Van Dyke and co-workers provided the detailed clinical description of some kindred that showed generalized motor seizures, in addition to typical EA1 symptoms [1]. The subsequent genetic analysis revealed that these individuals carried the F184C mutation in their *KCNA1* gene [6]. The functional characterization of F184C channels in *Xenopus* oocytes and mammalian cells showed that this mutation right shifted the mid-point of channel activation and slowed ~2-fold the time constants of activation [12–14]. This phenylalanine to cysteine substitution at position 184 is located in the carboxy-terminal portion of the first transmembrane domain (S1). Recent reports suggested that the S1 segment plays a critical role in Kv1.1 channel function. It has been proposed that helix–helix interactions may take place between the S1 and the nearby segments and affect the activation–deactivation kinetics and voltage-dependence of this channel type [15,16].

Kv1.1 or *Shaker*-like potassium channels are modulated by several intracellular and extracellular factors, including Zn^{2+} ions [17–19]. This inorganic ion is relatively abundant in the brain (approximately 100–350 μM) and widely distributed through the CNS [20,21]. Zn^{2+} can be stored in vesicles and released from presynaptic terminals by means of exocytosis. The presynaptic vesicles of glutamatergic terminals contain millimolar concentrations of Zn^{2+} [20], which could reach transiently 100–300 μM or higher in the local microenvironment during release [22,23]. In particular, Zn^{2+} is released from mossy fiber terminals in the hippocampus and from the basket cell terminals of the cerebellum where Kv1.1 channels are also expressed [22,24–26]. An altered sensitivity to Zn^{2+} may therefore have a profound effect on hKv1.1 function.

Structural studies of several zinc-binding proteins demonstrate that zinc is typically coordinated by histidine, cysteine, and less commonly, aspartate and glutamate residues. Therefore, the main aim of the study was to investigate whether the F184C mutation may alter the Zn^{2+} sensitivity of the channel.

---

* Corresponding author. Fax: +39-075-5857371.
E-mail address: pessia@unipg.it (M. Pessia).

[1] Present address: Istituto di Biomedicina e Immunologia Molecolare, CNR,via Ugo La Malfa 153, 90146 Palermo.

Abbreviations: MTSEA, (2-aminoethyl) methane thiosulfonate; MTSES, (2-sulfonatoethyl) methane thiosulfonate; MTSET, (2-trimethylammoniumethyl) methane thiosulfonate

Indeed, we find that F184C channels showed a higher affinity for zinc than the wild-type (WT) and the activation kinetics of the mutated channel were markedly slowed by this metal ion. The data demonstrate that zinc alters the gating properties of F184C channel that may contribute to causing EA1 symptoms in patients bearing this genetic mutation.

2. Materials and methods

2.1. Heterologous expression of Kv channels in Xenopus oocytes

Procedures involving Xenopus laevis and their care have been conducted in conformity with the institutional guidelines that are in compliance with national (D.L. no. 116, G.U., suppl. 40, 18 February, 1992) and international laws and policies (EEC Council Directive 86/609, OJ L 358,1, Dec. 12, 1987; NIH Guide for the Care and Use of Laboratory Animals, NIH Publication No. 85-23, 1985 and Guidelines for the Use of Animals in Biomedical Research, Thromb. Haemost. 58, 1078–1084, 1987).

The animals underwent no more than two surgeries, with an interval of at least three weeks. Xenopus laevis were anesthetized with an aerated solution containing 5 mM 3-aminobenzoic acid ethyl ester methansulfonate salt and 60 mM sodium bicarbonate, pH 7.3. The ovary was dissected and the oocytes digested in OR-2 solution containing 0.5 units/ml collagenase A (SIGMA). In vitro transcribed mRNAs were microinjected into the oocytes 24 h later by using a nanoliter injector-WPI and incubated at 16 °C. Typically, every oocyte was injected with 50 nl of a solution containing the relevant mRNA. The amount of the mRNAs was quantified using a spectrophotometer and by ethidium bromide staining.

2.2. Electrophysiology

Two-electrode voltage-clamp recordings (TEVC) were performed from Xenopus oocytes at ~22 °C, 1–8 days after injection. A Gene-Clamp 500 amplifier (Axon Instruments) interfaced to a Power Macintosh 7200/90 computer with an ITC-16 interface (Instrutech Corp., New York, USA) was used. Microelectrodes were filled with KCl 3 M and had resistances of 0.1–0.5 MΩ. The recording solution contained (mM): NaCl 96, KCl 2, MgCl$_2$ 1, CaCl$_2$ 1.8, and HEPES 5, pH 7.4. Currents were evoked by voltage commands from a holding potential of −80 mV as described in the figure legends. Tail currents were fitted with a double exponential function and the amplitude was calculated to determine the peak tail currents. The recordings were filtered at 2 kHz and acquired at 5 kHz with a Pulse software (HEKA elektronik GmbH, Germany). Data analysis was performed by using: IGOR (Wavemetrics), PulseFit (HEKA elektronik GmbH, Germany) and KaleidaGraph (Synergy Software, USA). Leak and capacitive currents were subtracted using a P/4 protocol. To determine the statistical significance, an unpaired Student's test was used. P values <0.01 were considered significant.

2.3. Molecular biology

The F184C mutation was introduced into the human Kv1.1 cDNA by using the QuikChange™ Site-Directed Mutagenesis Kit (Stratagene) according to the manufacturer's instructions. The nucleotide sequence of the mutant subunit was determined by automated sequencing. All cDNAs were subcloned into the oocyte expression vector pBF, which provides 5′ and 3′ untranslated regions from the Xenopus β-globin gene, flanking a polylinker containing multiple restriction sites. The cRNAs were synthesized in vitro by using SP6 RNA polymerase.

3. Results

3.1. The F184C mutation increases the sensitivity of the channel to Zn²⁺-induced inhibition

In order to determine the sensitivity of F184C channels to Zn^{2+}, this point mutation was introduced into the human Kv1.1 cDNA by site-directed mutagenesis and in vitro transcribed mRNA microinjected into Xenopus oocytes. The

macroscopic currents were recorded from oocytes expressing WT and F184C channels under two-electrode voltage-clamp configuration, before and during the superfusion into the recording chamber of a solution containing ZnCl$_2$ (Fig. 1). These recordings revealed that indeed F184C currents were reduced significantly more than the WT by Zn^{2+}. To determine the K_D for Zn^{2+} inhibition of WT and F184C channels, the concentration–response relationships were constructed at +60 mV. This test potential was chosen for two main reasons: (i) the open probability of WT and F184C channel is maximal at this potential [27,14] and, therefore, both channel types have been exposed to the same concentrations of zinc when their overall activity is similar; (ii) this potential corresponds approximately at the peak of the action potential and it allows to gain physiologically relevant information. This analysis revealed that the F184C mutation increases ~4.5-fold the K_D for Zn^{2+} reduction of the current amplitude (Fig. 2C).

Wild-type hKv1.1 channels possess a native cysteine at position 185. To test the contribution of this residue to Zn^{2+}-induced current reduction, the C185 was mutated into an alanine in both WT and F184C channels. The Zn^{2+} concentration–inhibition relationships for C185A and F184C/C185A channels yielded K_D values of 1.8 ± 0.1 mM (Hill coefficient: 0.8) and 5.1 ± 0.4 mM (Hill coefficient: 0.8), respectively (mean $\pm$ S.E.M. of 4–6 cells). These results suggest that the sensitivity of the channel to Zn^{2+} is not abolished by mutation of the cysteine at position 185.

3.2. Effects of Zn²⁺ and Cd²⁺ on the activation–deactivation kinetics and on the voltage dependence of F184C channels

Zn^{2+} ions are known to modulate the activation–deactivation kinetics of voltage-gated potassium channels. To deter-
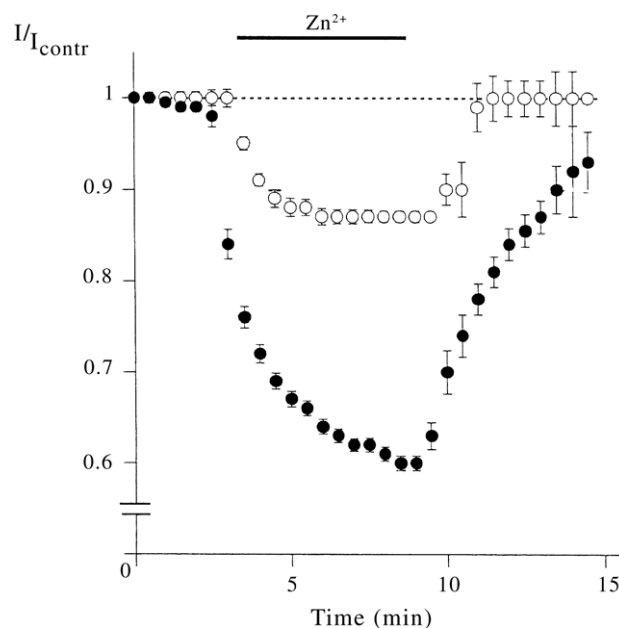

Fig. 1. Current inhibition induced by Zn^{2+} on hKv1.1 WT and F184C currents The data points show the effects of Zn^{2+} on the normalized current amplitudes recorded at +60 mV (interpulse interval: 30 s) from Xenopus oocytes expressing WT (○) and F184C (●) channels. The bar above the records indicates the period during which the perfusing solution was changed to one that contained Zn^{2+} 1 mM (mean $\pm$ S.E.M. of 6 cells).
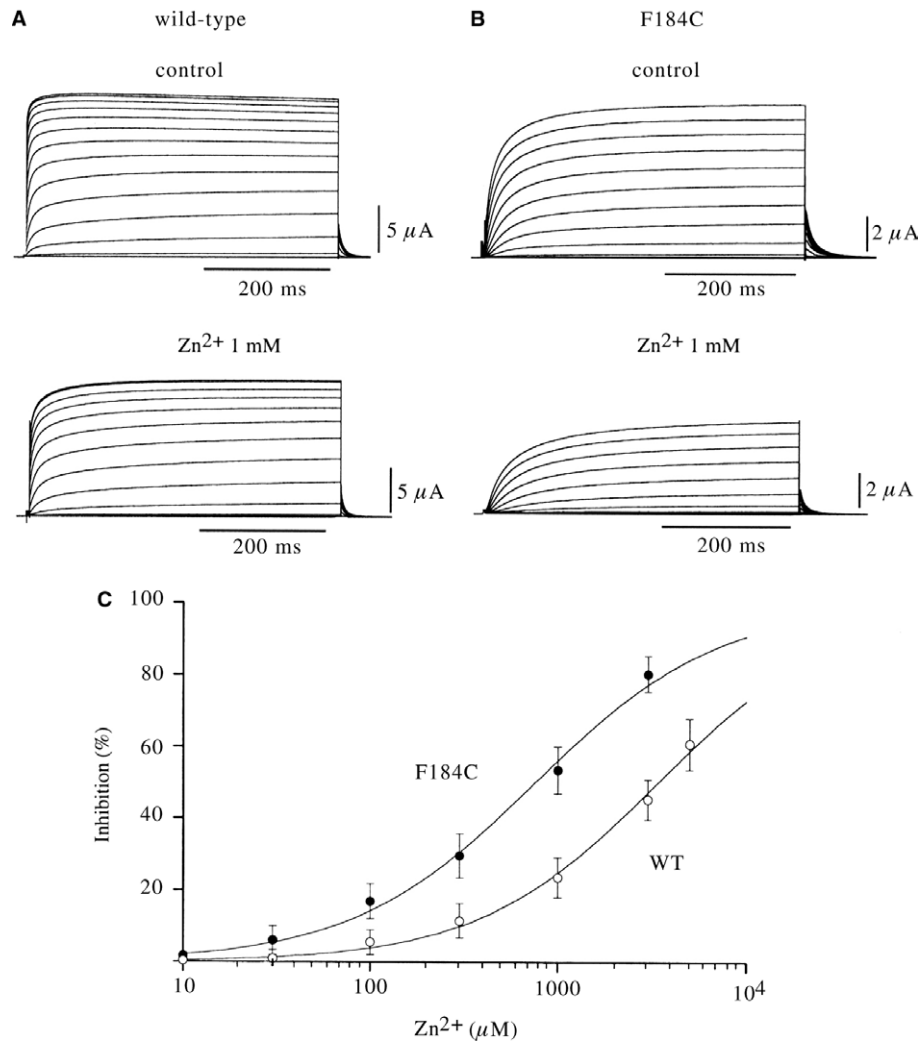
Fig. 2. F184C channels show a higher sensitivity to Zn^{2+}-induced inhibition. Representative current families recorded from *Xenopus* oocytes expressing the indicated channels before (above) and after (below) the superfusion of 1 mM Zn^{2+} (A and B). The currents were evoked by 500 ms depolarizing commands from −60 to +60 mV, delivered in 10 mV increments from a holding potential of −80 mV. (C) Concentration–response relationships for Zn^{2+} inhibition of WT (○) and F184C (●) steady-state current recorded at +60 mV. The solid lines represent the fit of the data points with the Hill equation yielding K_D values of 3.4 ± 0.2 mM (Hill coefficient: 0.9) and $0.75 \pm 0.01^*$ mM (Hill coefficient: 0.9) for WT and F184C channels, respectively ($^*P < 0.01$; mean $\pm$ S.D.; $n = 6$).

mine whether the F184C mutation alters the Zn^{2+}-modulation of the channel's kinetics, the activation and deactivation time constants were calculated at several potentials before and after the external application of 30 μM Zn^{2+}, and plotted as a function of membrane potentials (Fig. 3). Zn^{2+} greatly slowed the kinetics of activation of F184C channels, but, did not affect their deactivation rates (Fig. 3B; see figure legend). The kinetics properties of WT channels were not modified significantly by 30 μM Zn^{2+} (Fig. 3A). The activation and deactivation time constants for WT and F184C channels were also calculated at different Zn^{2+} concentrations (Fig. 4). These results revealed that Zn^{2+} markedly increases the time constants of F184C activation, in a concentration dependent fashion (Fig. 4A). By contrast, the time constants of WT channel activation were little affected even at very high Zn^{2+} concentrations. On the other hand, Zn^{2+} accelerated the deactivation rates of WT and F184C channels, similarly (Fig. 4B).

Some Zn^{2+}-induced effects can be exerted also by cadmium ions. To assess the effects of Cd^{2+} on F184C kinetics, the activation and deactivation time constants were calculated at several potentials before and after the external application of 500 μM $CdCl_2$ and plotted as a function of membrane potentials (Fig. 5A). This plot shows that Cd^{2+} greatly slowed the kinetics of activation of F184C channels. By contrast, the deactivation rates were slightly accelerated by Cd^{2+}. The kinetics properties of WT channels were not modified significantly by this divalent cation (Fig. 5A inset; see figure legend).

Cd^{2+} (500 μM) also shifted the $V_{1/2}$ of F184C channels ~ 32 mV to positive potential and did not modify the slope factor k (Fig. 5B). On the other hand, the current–voltage relationship of WT channels was right-shifted ~ 10 mV by cadmium (not shown). Four of such experiments were carried out independently and yielded similar results. The shift caused by Cd^{2+} on F184C voltage-dependence suggested that Zn^{2+} might consequently exert a similar effect (Fig. 6).
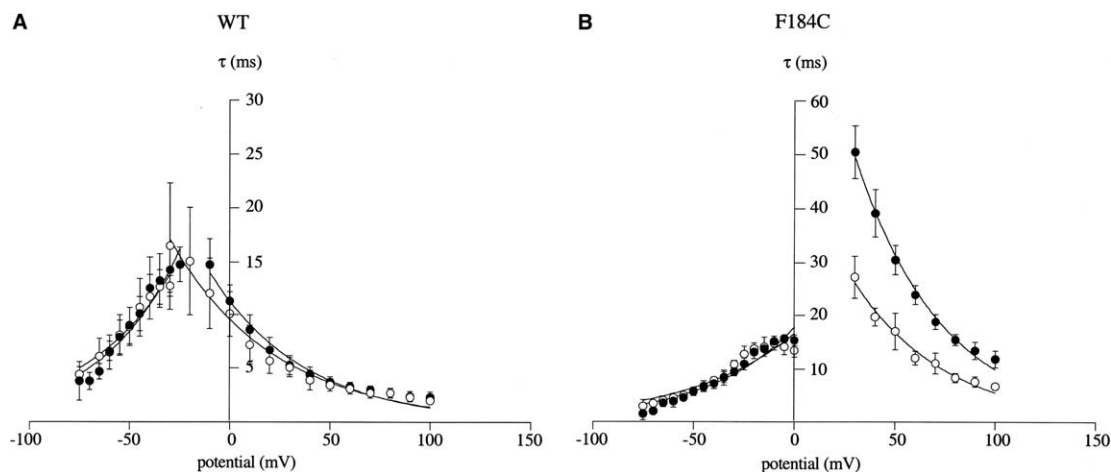
Fig. 3. Zn^{2+} slows the activation rates of F184C channels at low micromolar concentrations. The activating and deactivating current traces for WT (A) and F184C (B) were recorded before (○) and after the application of 30 µM Zn^{2+} (●). The activating currents were evoked as described in Fig. 2. The deactivating currents were recorded after a depolarizing command to +60 mV for 200 ms duration, followed by hyperpolarizing test commands delivered in 10 mV decrements in a voltage range between +60 and −80 mV. The activating and deactivating current traces were fitted with two exponential functions. The fast time constants were plotted as a function of membrane potential and were fitted with the equation: $\tau = \tau_{V_{1/2}} \exp[(V - V_{1/2})/k]$, where $\tau_{V_{1/2}}$ is the time constant at the $V_{1/2}$ of each channel type and k is the slope factor for the voltage dependence of the time constants. The data points are means ± S.E.M. of 6–7 cells. The $\tau_{V_{1/2}}$ (ms) and the slope factors k (mV; in brackets) were for WT channels, $WT_{control}$: activation 16.4 ± 0.4 (52.1 ± 2.3), deactivation 14.4 ± 0.5 (44.5 ± 3.9); WT_{zinc}: activation 20.5 ± 1.1 (46.7 ± 2.7), deactivation 14.9 ± 0.6 (38.7 ± 3.4). For F184C channels these values were $F184C_{control}$: activation 52.3 ± 3.7 (44.8 ± 2.8), deactivation 16.0 ± 0.9 (52.6 ± 5.9); $F184C_{zinc}$: activation 101.0 ± 4.3* (43.2 ± 1.5), deactivation 17.0 ± 0.7 (43.8 ± 3.3). *Significance of $P < 0.01$ compared with control.
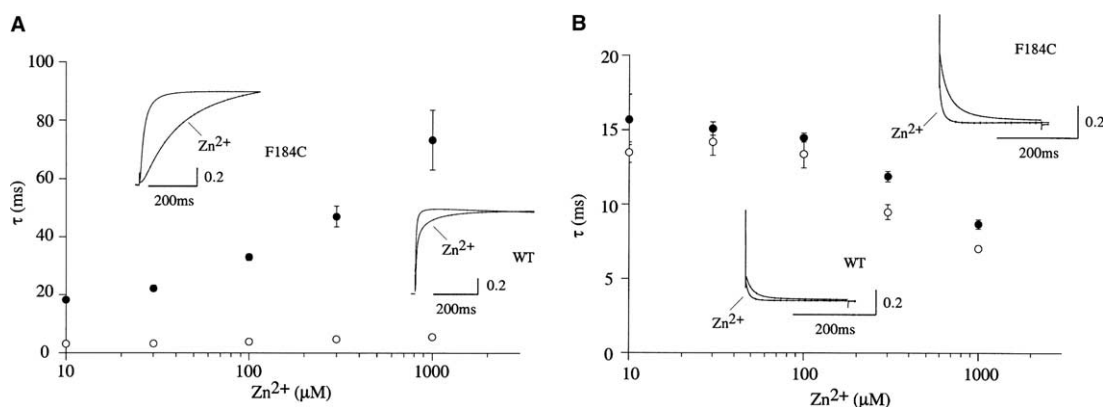

Fig. 4. Concentration-dependent effects of Zn^{2+} on the activation and deactivation of WT and F184C channels. (A) Fast time constant of activation calculated at +60 mV for WT (○) and F184C channels (●) and plotted as a function of zinc concentration. The insets show superimposed and normalized current traces recorded at +60 mV before and after the application of Zn^{2+} (300 µM) from oocytes expressing the indicated channels. (B) The fast time constants of deactivation were calculated at −30 mV for WT (○) and at 0 mV for F184C channels (●) and plotted as a function of zinc concentration. These potentials correspond approximately at the $V_{1/2}$ of each channel type. The insets show the deactivating current traces recorded before and after the application of Zn^{2+} (300 µM) from oocytes expressing the indicated channels. The data points are means ± S.E.M. of 6–7 cells.

Indeed, the current–voltage relationships for F184C were right-shifted also by Zn^{2+}. This effect was more pronounced for F184C than for WT channels. The shift of the midpoint activation voltage ($V_{1/2}$), caused by Zn^{2+} on both channel types, was concentration dependent (Fig. 6C). The Zn^{2+} concentration–response curve was shifted leftward for F184C channels and yielded a half-maximal concentration significantly different from that of WT channels (Fig. 6, see figure legend).

A number of control experiments were carried out to assess the contribution of divalent cation effect by using external solutions containing both 5 mM Mg^{2+} and 4 mM Ca^{2+} [28]. The effects of Zn^{2+} on current amplitudes, kinetics and voltage-dependence of F184C channels were not prevented by

solutions containing both calcium and magnesium at higher concentrations.

3.3. The carboxy-terminal region of S1 is accessible to MTS reagents

Methanethiosulfonate (MTS) are cysteine-modifying reagents that have been extensively used in site-specific accessibility studies of ion channels [29]. Generally, it is assumed that the hydrophilic MTS compounds, which also bear a positive or negative charge, react rapidly with a cysteine that is exposed to either the intracellular or extracellular milieu. Therefore, we tested the reactivity of the F184C channel with the (2-aminoethyl) methane thiosulfonate (MTSEA), (2-sulfonatoethyl) methane thiosulfonate (MTSES) or (2-trime-
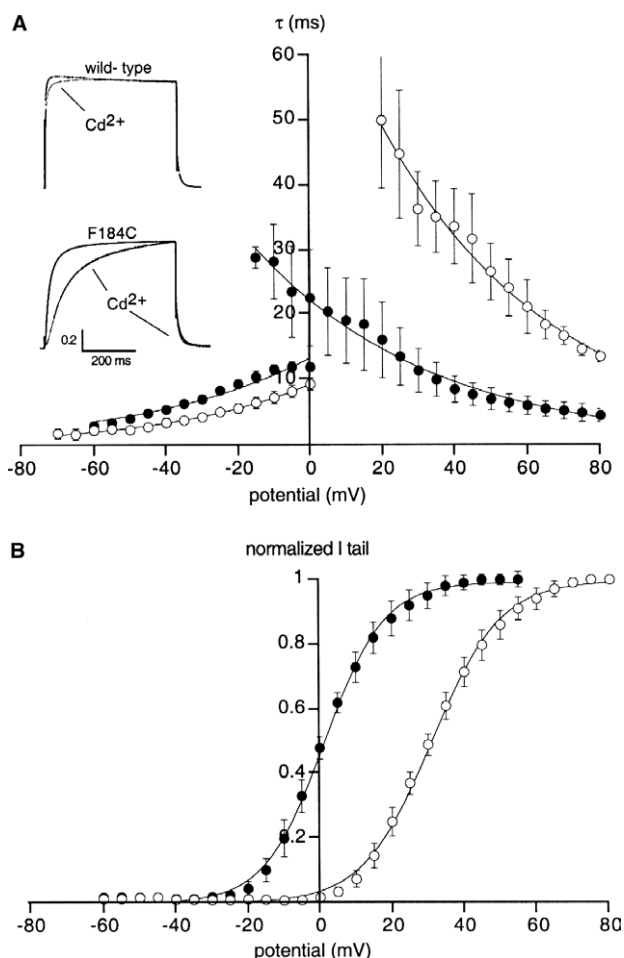
Fig. 5. Cadmium ions affect the kinetics and voltage-dependence of F184C channels. (A) The insets show the superimposed and normalized current traces recorded at +20 mV from *Xenopus* oocytes expressing the indicated channels, before and after the application of 500 µM cadmium. The activating and deactivating F184C current traces were fitted with double exponential functions and the fast time constants were calculated before (●) and after the application of 500 µM Cd^{2+} (○). The solid lines show the fit of the data points (mean ± S.D. of 7 cells) with the equation: $\tau = \tau_{V_{1/2}} \exp[(V - V_{1/2})/k]$, where $\tau_{V_{1/2}}$ is the time constant at the $V_{1/2}$ of the channel and k is the slope factor for the voltage dependence of the time constants. The time constants calculated at the activation midpoint ($\tau_{V_{1/2}}$; ms) and the slope factors k (mV; in brackets) were for F184C channels, F184C$_{control}$: activation 22.1 ± 0.3 (48.8 ± 1.5), deactivation 26.2 ± 1.9 (46.8 ± 3.2); F184C$_{cadmium}$: activation 39.4 ± 0.5* (47.7 ± 1.8), deactivation 20.5 ± 0.5 (40.2 ± 0.8). For WT channels these values were WT$_{control}$: activation 7.2 ± 0.1 (32.9 ± 1.3), deactivation 20.1 ± 1.0 (29.1 ± 1.5); WT$_{cadmium}$: activation 11.7 ± 0.4 (33.7 ± 2.3), deactivation 23.5 ± 1.0 (33.8 ± 2.0); mean ± S.D., $n = 7$. *Significance of $P < 0.01$ compared with control. (B) The current–voltage relationships of F184C channels were constructed before (●) and after the extracellular application of 500 µM Cd^{2+} (○). The normalized peak tail currents were plotted as a function of membrane prepulse potentials and fitted with a Boltzmann function: $I = 1/\{1 + \exp[(V - V_{1/2})/k]\}$ from which the $V_{1/2}$ and k values were computed. The I–V data points are means ± S.D. of 7 cells.

Fig. 6. Zn^{2+}-modulation of WT and F184C voltage-dependence. The peak tail currents were recorded from oocytes expressing WT (A) and F184C channels (B) before (●), during the superfusion of 1 mM Zn^{2+} (○) and after its wash-out from the recording chamber (♦). These currents were normalized, plotted as a function of membrane prepulse potentials and fitted with a Boltzmann function (solid line). The insets show representative I–Vs before normalization for WT and F184C channels where the current reduction is also obvious after the application of 1 mM Zn^{2+} (○). (C) Concentration-dependent effects of Zn^{2+} on the delta mid-point activation curve for WT (○) and F184C channels (●). The solid lines represent the fit of the data points with a Hill equation yielding a half-maximal concentration of Zn^{2+} of 500 ± 45 µM (Hill coefficient: 1) and 286 ± 45* µM (Hill coefficient: 0.8) for WT and F184C channels, respectively (mean ± S.D. of 6–7 cells). *Significance of $P < 0.01$ compared with WT.

thylammoniumethyl) methane thiosulfonate (MTSET) compounds. Several control experiments showed that the superfusion of solutions containing 0.1–5 mM MTSEA, MTSES or MTSET onto *Xenopus* oocytes expressing WT channels, did not alter the voltage-dependence and amplitude of the currents (Fig. 7, left panels). By contrast, the application of
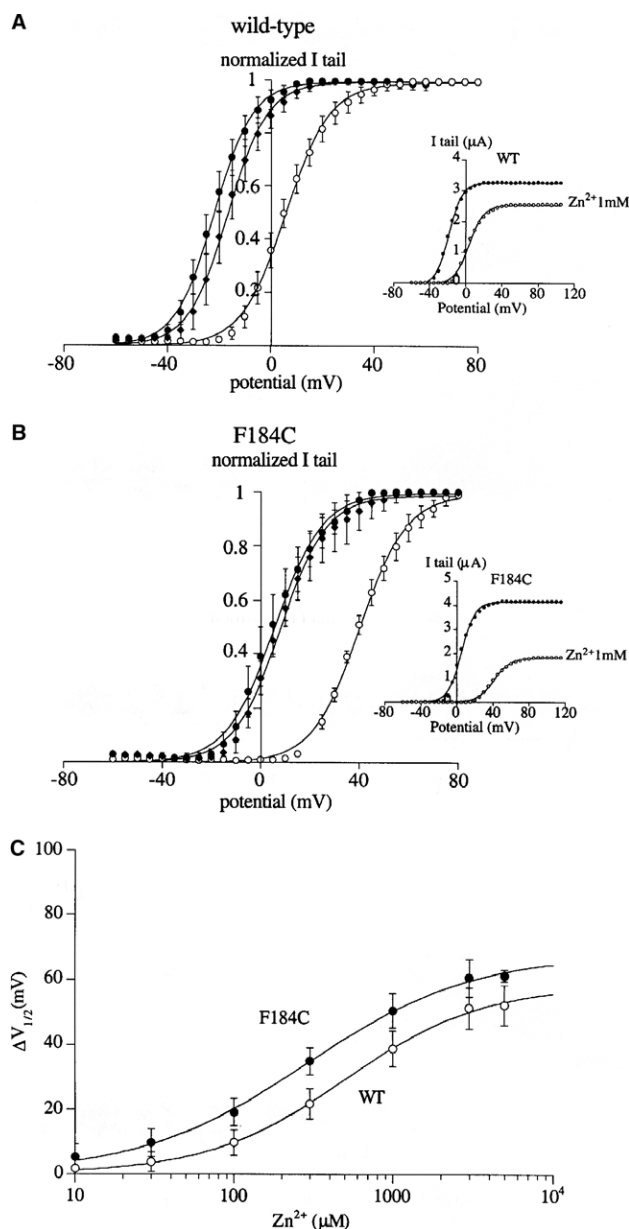
the positively charged MTSEA (100 µM), shifted the midpoint activation voltage of F184C channels ∼39 mV to the right, leaving their slope factor k unaltered (Fig. 7B; Table 1). The effects exerted by MTSES 100 µM was much less pronounced (Fig. 7D; Table 1). On the other hand, the
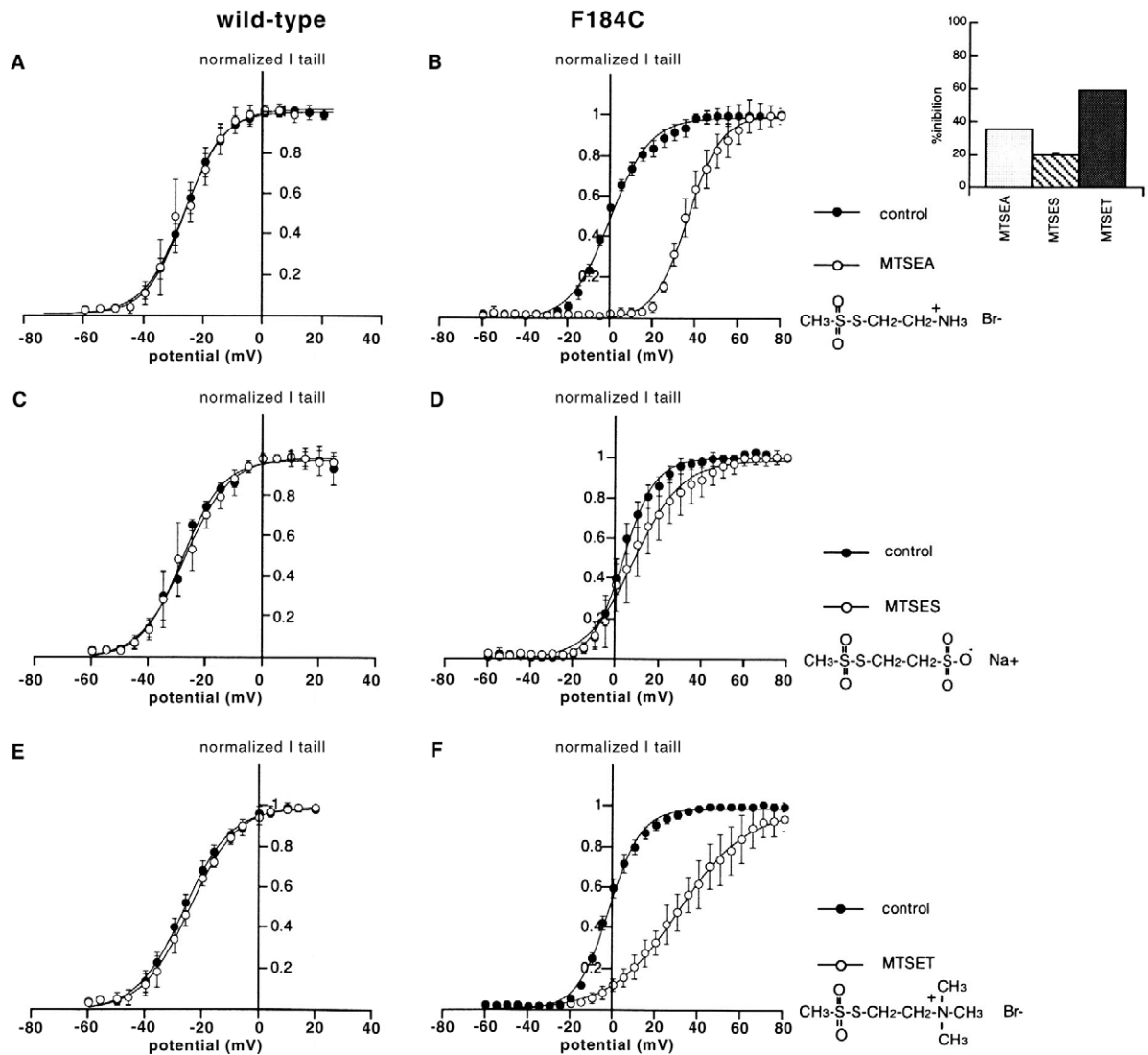
Fig. 7. The carboxy-terminal region of S1 is accessible to MTS-reagents. Current-voltage relationships of WT channels obtained in control conditions (●) and after the extracellular application of MTSEA, MTSES and MTSET (100 μM/10 min, ○; left panels). The right panels show the I–Vs for F184C before (●) and after the superfusion of the indicated sulfhydryl reagents (100 μM/10 min, ○). The I–Vs were constructed as detailed in Fig. 5. The inset shows the inhibitory effects exerted by the indicated MTS-derivatives on F184C currents. The bar graph reports the maximal current inhibition (%) calculated at +60 mV. WT current amplitudes were not affected by the superfusion of these compounds (not shown).

Table 1
Effects of MTS-reagents on the voltage-dependent parameters of WT and F184C channels

	WT		F184C	
	$V_{1/2}$ (mV)	k (mV)	$V_{1/2}$ (mV)	k (mV)
Control	-27.0 ± 2.0	7.2 ± 1.3	-1.8 ± 1.4	7.7 ± 0.7
MTSEA	-27.8 ± 1.2	7.8 ± 2.1	$36.8 \pm 3.2^*$	7.4 ± 2.0
MTSES	-27.4 ± 3.2	7.9 ± 0.9	$9.4 \pm 7.5^*$	$10.6 \pm 2.2^*$
MTSET	-26.4 ± 3.0	6.2 ± 0.8	$31.7 \pm 7.4^*$	$15.9 \pm 2.8^*$

The voltage-dependent parameters of activation were calculated from the Boltzmann equation that was fitted to the current–voltage data points plotted in Fig. 7. The data are means ± S.D. of 7 cells.
* Significance of $P < 0.01$ compared with control.

superfusion of MTSET (100 μM) produced a shift of the voltage-dependence of F184C channel that was similar to that exerted by MTSEA and, in addition, increased ∼2-fold the slope factor k (Fig. 7F; Table 1). The F184C current amplitude was reduced by the MTS-compounds differently

(Fig. 7, inset). The effects produced by these reagents on both the voltage-dependence and amplitude of F184C currents were irreversible and were not observed in the presence of dithiothreitol (10 mM), confirming the high specificity of these reactions (not shown).

4. Discussion

In this study, we demonstrate that the episodic ataxia mutation F184C confers Kv1.1 channels with a higher sensitivity to zinc. The Zn^{2+}-induced current decrease, its effects on the kinetics of activation and on the voltage-dependence of the channel likely contribute to the EA1 symptoms observed in patients carrying the F184C mutation.

4.1. Pathogenic implications for EA1 syndrome and other genetic diseases

Voltage-gated potassium channels (Kv) play key roles in neurotransmission and nerve cell physiology. In particular, these ion channels keep action potentials short and modulate the release of neurotransmitters. They also control the excitability, the electrical properties and the firing pattern of central and peripheral neurons [30].

Here, we show that Zn^{2+} ions inhibit F184C currents at concentrations significantly lower than those required to inhibit WT channels. In addition, Zn^{2+} greatly slows the kinetics of F184C channel activation and speeds up the rate of deactivation. By contrast, the rates of WT channels activation are relatively insensitive. Moreover, Zn^{2+} positively shifts the voltage dependence of activation in a concentration dependent fashion. This shift is more pronounced for F184C channels rather than for the WT. The Zn^{2+}-induced inhibition and its effect on the opening rate of the mutated channel is already significant at a lower micromolar range where this effect may become pathophysiologically relevant. Furthermore, the Zn^{2+} concentration response curves were constructed at +60 mV, the peak of the action potential (Fig. 2). However, the Zn^{2+} sensitivity of Kv1.1 channels is much higher at less depolarized potentials [17] and therefore the Zn^{2+}-induced reduction of F184C current amplitude is likely to be underestimated. This also suggests that the electrical events which depolarize nerve cell membranes to less positive values would be more affected by the same concentration of Zn^{2+}. During the vesicular release of Zn^{2+} its inhibitory actions on F184C channels will be additional to the intrinsic gating defects caused by the mutation itself. These combined effects of the F184C mutation are likely to result in increased cellular excitability. However, some nerve structures would be more hyperexcitable than others due to the additional Zn^{2+} effects. These would include the hippocampus and the basket cell terminals of the cerebellum where Kv1.1 channels likely undergo Zn^{2+}-modulation [22,24–26]. Interestingly, patients bearing F184C mutation showed generalized motor seizures, in addition to typical EA1 symptoms [1]. Whether Zn^{2+} plays any role in triggering epileptic like symptoms in these patients remains to be determined. On a more general note, these findings point out that any genetic disease introducing a cysteine or histidine mutation may affect the sensitivity of the mutated protein to Zn^{2+} as for F184C channels. Consequently, Zn^{2+} may alter the functional properties of the protein and contribute to the pathogenesis of the disease.

4.2. Speculations on Kv1.1 structure–function

The effects of Zn^{2+} on current amplitudes, kinetics and voltage-dependence of F184C channels were observed also in the presence of external solutions containing higher concentrations of divalent cations such as calcium and magnesium. This suggests that surface charge screening is an unlikely mechanism underlying the Zn^{2+}-induced effects on F184C channels [28,31]. At least to some extent, Zn^{2+} modulates WT channels as well. The molecular determinants of the Zn^{2+} effects on Kv1.1 channels are unknown. Recent studies on Kv1.5 channels have shown that Zn^{2+} may act on two distinct binding sites, one of which is located in the pore turret [32,33]. It is possible that similar binding sites for this metal ion could be found in both Kv1.1 and Kv1.5, although the latter channel type is far more sensitive to Zn^{2+} [19]. Whether the F184C mutation enhances the Zn^{2+} sensitivity of the channel by producing a novel Zn^{2+} binding site or by means of a different mechanism(s) remains to be established.

Zn^{2+} and Cd^{2+} specifically modulate F184C channel activity by shifting the mid-point of channel activation to more depolarized potentials. Some MTS reagents caused this shift as well. The rightward shift in the voltage dependence of activation suggests that Zn^{2+}, Cd^{2+} and the MTS reagents decrease the relative stability of the active conformation of the channel. Moreover, the slower opening and faster closing kinetics observed after the application of both Zn^{2+} and Cd^{2+} suggest that these ions may affect the conformational changes coupled to channel opening. In particular, it appears that the F184C mutation increases the Zn^{2+} and Cd^{2+}-induced stabilization of the closed channel conformation(s), thus, further delaying channel opening.

The cysteine-modifying reagents MTSEA, MTSET and MTSES affect both the current amplitudes and voltage dependence of F184C channels. These effects are either irreversible or do not occur in the presence of reducing agents. This site-specific accessibility evidence suggests that the carboxy-terminal region of the S1 segment: (i) should be exposed to the extracellular compartment either permanently or during the conformational rearrangements occurring upon channel gating or (ii) it resides in the interior of the membrane but, somehow, it is still accessible to MTS reagents. Interestingly, a recent report has also demonstrated the accessibility of the F184C residue in the related *Shaker* potassium channel [34]. The *Shaker* mutant F244C (which corresponds to F184C in hKv1.1) was shown to react with MTSET in both the open and closed conformation of the channel, demonstrating that the exposure of this residue is state independent [34]. However, MTSET caused a leftward shift of the F244C channel current–voltage relationship. By contrast, we observed a rightward shift of the F184C channel I/V. The reasons for this discrepancy are unknown. We have also shown that MTSET increases the slope factor of the activation curve for F184C channel. The calculated product of the gating charges of the channel z, times the fraction of the field that they traverse δ ($z\delta$ value) was reduced $\sim$2-fold by MTSET. In conventional models, this would suggest that MTSET impairs the conformational rearrangements that the voltage-sensing domains undergo upon membrane depolarization [35]. However, further experiments will be required to assert this with certainty.

5. Conclusions

These studies have allowed us to define an additional pathogenic mechanism in EA1, which likely exacerbates the symptoms in patients carrying F184C mutations. Furthermore, it should be kept in mind that genetic mutations

introducing histidine or cysteine residues may alter the zinc sensitivity of a given protein and, as a consequence, contribute to the pathogenesis of the disease.

References

[1] Van Dyke, D.H., Griggs, R.C., Murphy, M.J. and Goldstein, M.N. (1975) J. Neurol. Sci. 25, 109–118.

[2] Bouchard, J.P., Roberge, C., van Gelder, N.M. and Barbeau, A. (1984) Can. J. Neurol. Sci. 11, 550–553.

[3] Brunt, E.R.P. and van Weerden, T.W. (1990) Brain 113, 1361–1382.

[4] Gancher, S.T. and Nutt, J.G. (1986) Mov. Disord. 1, 239–253.

[5] Browne, D.L., Gancher, S.T., Mutt, J.G., Brunt, E.R.P., Smith, E.A., Kramer, P. and Litt, M. (1994) Nat. Genet. 8, 136–140.

[6] Browne, D.L., Brunt, E.R.P., Griggs, R.C., Nutt, J.G., Gancher, S.T., Smith, E.A. and Litt, M. (1995) Hum. Mol. Genet. 4, 1671–1672.

[7] Comu, S., Giuliani, M. and Narayanan, V. (1996) Ann. Neurol. 40, 684–687.

[8] Litt, M., Kramer, P., Browne, D., Gancher, S., Brunt, E.R.P., Root, D., Phromchotikul, T., Dubay, C.J. and Nutt, J. (1994) Am. J. Hum. Genet. 55, 702–709.

[9] Ashcroft, M.F. (1999) Ion Channels and Disease. Academic Press, San Diego, USA.

[10] Kullmann, D.M., Rea, R., Spauschus, A. and Jouvenceau, A. (2001) Neuroscientist 7, 80–88.

[11] D'Adamo, M.C., Imbirici, P. and Pessia, M. (2002) in: (Manto, M., Pandolfo, M., Eds.), pp. 562–572, Cambridge University Press.

[12] Adelman, J.P., Bond, C.T., Pessia, M. and Maylie, J. (1995) Neuron 15, 1449–1454.

[13] Zerr, P., Adelman, J.P. and Maylie, J. (1998) J. Neurosi. 18, 2842–2848.

[14] Bretschneider, F., Wrisch, A., Lehmann-Horn, F. and Grissmer, S. (1999) Eur. J. Neurosci. 11, 2403–2412.

[15] Mathur, R., Zhou, J., Babila, T. and Koren, G. (1999) J. Biol. Chem. 274, 11487–11493.

[16] Imbrici, P., Cusimano, A., D'Adamo, M.C., De Curtis, A. and Pessia, M. (2003) Pflügers Arch. 446, 373–379.

[17] Harrison, N.L., Radke, H.K., Tamkun, M.M. and Lovinger, D.M. (1993) Mol. Pharmacol. 43, 482–486.

[18] Harrison, N.L. and Gibbons, S.J. (1994) Neuropharmacology 33, 935–952.

[19] Zhang, S., Kwan, D.C., Fedida, D. and Kehl, S.J. (2001) J. Physiol. 532, 349–358.

[20] Frederickson, C.J. (1989) Int. Rev. Neurobiol. 31, 145–238.

[21] Weiss, J.H., Sensi, S.L. and Koh, J.Y. (2000) Trends Pharmacol. Sci. 21, 395–401.

[22] Assaf, S.Y. and Chung, S.H. (1984) Nature 308, 734–736.

[23] Howell, G.A., Welch, M.G. and Frederickson, C.J. (1984) Nature 308, 736–738.

[24] Wang, H., Kunkel, D.D., Schwartzkroin, P.A. and Tempel, B.L. (1994) J. Neurosci. 14, 4588–4599.

[25] Wang, Z., Danscher, G., Kim, Y.K., Dahlstrom, A. and Mook Jo, S. (2002) Neurosci. Lett. 321, 37–40.

[26] Rhodes, K.J., Strassle, B.W., Monaghan, M.M., Bekele-Arcuri, Z., Matos, M.F. and Trimmer, J.S. (1997) J. Neurosci. 17, 8246–8258.

[27] D'Adamo, M.C., Liu, Z., Adelman, J.P., Maylie, J. and Pessia, M. (1998) EMBO J. 17, 1200–1207.

[28] Spires, S. and Begenisich, T. (1992) J. Gen. Physiol. 100, 181–193.

[29] Karlin, A. and Akabas, M.H. (1998) Methods Enzymol. 293, 123–145.

[30] Hille, B. (2001) 2nd edn., Sinauer, Sunderland, MA.

[31] Gilly, W.F. and Armstrong, C.M. (1982) J. Gen. Physiol. 79, 965–996.

[32] Zhang, S., Kehl, S.J. and Fedida, D. (2001) Biophys. J. 81, 125–136.

[33] Kehl, S.J., Eduljee, C., Kwan, D.C., Zhang, S. and Fedida, D. (2002) J. Physiol. 541, 9–24.

[34] Gandhi, C.S., Clark, E., Loots, E., Pralle, A. and Isacoff, E.Y. (2003) Neuron 40, 515–525.

[35] Bezanilla, F. (2000) Physiol. Rev. 80, 555–592.